

Article

A Complicated Karst Spring System: Identified by Karst Springs Using Water Level, Hydrogeochemical, and Isotopic Data in Jinan, China

Yi Guo ^{1,2,3} , Dajun Qin ^{1,2,3,4,*}, Lu Li ^{1,2,3}, Jie Sun ^{1,2,3}, Fulin Li ⁵ and Jiwen Huang ⁵

¹ Key Laboratory of Shale Gas and Geoenvironment, Institute of Geology and Geophysics, Chinese Academy of Sciences, Beijing 100029, China; cugguoyi@163.com or guoyi@mail.iggcas.ac.cn (Y.G.); liluiggcas@sina.cn (L.L.); jie.s@mail.iggcas.ac.cn (J.S.)

² Institutions of Earth Science, Chinese Academy of Sciences, Beijing 100029, China

³ University of Chinese Academy of Sciences, Beijing 100049, China

⁴ Academician Zhaiming Guo working station, Sanya University, Hainan 572000, China

⁵ Water Resources Research Institute of Shandong Province, Ji'nan 250013, China; fulinli@126.com (F.L.); sdskyhjw@126.com (J.H.)

* Correspondence: qindj@mail.iggcas.ac.cn; Tel.: +86-010-8299-8589

Received: 27 March 2019; Accepted: 30 April 2019; Published: 6 May 2019



Abstract: The Jinan karst spring system, discharged by 108 springs in 2.6 km² city center area of Jinan, China, has been suffering lower regional groundwater levels, which threatens the karst springs outflowing and aquatic ecological civilization. For better spring protection, monthly hydrogeochemical and isotopic investigations were conducted in four representative karst springs (Baotu Spring (BTQ), Heihu Spring (HHQ), Zhenzhu (ZZQ), and Wulongtan Springs (WLT)) in 2016. Results showed that the BTQ, WLT, and ZZQ had similar hydrogeochemical and isotopic behaviors, which were different with that of HHQ. By combining the daily water level data with monthly hydrogeochemical and isotopic data of BTQ and HHQ, the hydrogeological processes of the two neighboring karst springs (470 m apart) are distinguished. (a) BTQ is recharged by two sources of precipitation and river water, while HHQ is recharged mainly by precipitation. (b) Hydrogeochemical characteristics of Baotu Spring are mainly controlled by calcite, dolomite, and gypsum dissolution mixture with river water and agricultural activity, while the hydrogeochemical characteristics of Heihu Spring are mainly controlled by calcite, dolomite, and gypsum dissolution in dry season, and dilution in wet season. (c) The discharge component of both springs is storage water by diffuse flow which is pressured by new infiltration rain water. The ratio of rain water is 14% in Baotu Spring and 9% in Heihu Spring calculated by a binary mixture model. Overall, this study puts forward the standpoint that neighboring karst springs with the same geological condition, can show different hydrogeological characteristics, which is a useful evidence for understanding the heterogeneity/complexity of karst aquifers.

Keywords: karst spring; hydrogeochemistry; stable isotope; water level; Jinan; China

1. Introduction

Karst aquifers crop out in approximately 12% of the global land surface and offer water resource for almost 25% of the world population [1–4]. In the past several decades, karst systems have been widely studied in aspects of the conceptual model [5–7], recharge sources [8–10], flow types [11,12], hydrogeochemical processes [13–21], hydrodynamics [22–24], responses to climate changes [25–27], and numerical modeling [28–30]. However, the heterogeneity and anisotropy of karst conduits and fractures created by uneven groundwater flow give rise to the complex hydrogeological conditions and make it difficult to understand and characterize the karst system [4,31,32].

The groundwater in karst aquifers generally discharges back to surface through one large spring or from a closely spaced spring cluster [33]. The hydrogeochemical and hydrodynamic characteristics of karst springs are the proxy for studying the unexploited karst aquifers [34,35], such as recharge processes [33,36–38], flow types [39], and system partition [40]. The springs exposing in the same area may be from different recharge zones through different drainages controlled by internal structural [4]. For example, two karst springs, a few meters apart in Mendip Hills in southwest England, were found to belong to two discrete conduit flow systems by tracer test [41]. Different flow paths of two neighboring karst springs in Cent Font, France were revealed with Pb isotopic compositions [42]. The complex hydrogeological process in a karst aquifer could attribute to the distinctive characteristics of neighboring springs, in return, the different behaviors of neighboring springs could also reflect the complexity of the karst aquifer system. Filippini et al. (2018) [43] found three nearby karst springs had different chemical characteristics at low-flow condition in Cansiglio-Monte Cavallo, Italy, due to a different recharge area. Mudarra and Andreo (2011) [44] found three neighboring springs responded to precipitation differently in Cadena carbonate aquifer in Southern Spain due to different recharge processes.

Bakalowicz et al. (2005) [3] and Hartmann et al. (2014) [2] summarized the major methods used for karst aquifer investigation, which are broadly classified into hydrodynamic analyses, hydrogeochemistry methods, and isotope methods. The hydrodynamics analyses of karst aquifers have been in great part based the spring hydrograph analyses [45]. The shapes of spring hydrographs are directly related to the hydraulic and transport properties of the karst aquifer, and are used to delineate the karst flow system [38], such as the flow processes [46], flow types [41], and flow components separation [47]. For example, Dreiss [48] used the linear kernel function identified by the spring hydrograph to characterize the karst aquifer.

Hydrogeochemistry of a karst spring is a useful tool for studying the hydrogeochemical processes in a karst aquifer based on the kinetic study of carbonate reactions and ion ratio [34,49]. Shuster and White [39] use the chemigraphs of several karst springs to reveal the flow type in a karst aquifer. Luo (2018) [38] used the chemigraphs of karst springs to divide the whole karst system into several vertically separated systems.

Oxygen and hydrogen isotopes of karst springs are considered as conservative tracers to characterize the conceptual hydrogeological model of karst aquifers [50], such as to identify the recharge area [22,51–53], determine the recharge amount [8], reveal the responses to rainfall event [54], separate the groundwater flow components [55], and estimate the aquifer storage [32].

Jinan karst system is one of the typical karst spring systems in North China, discharging by 108 springs in 2.6 km² of the city center. Earlier studies for Jinan karst springs were mainly focused on the hydrodynamic responses to exploitation [56,57] or rainfall [58,59], and the hydrochemical characteristic [60]. These studies considered the springs as the same although some differences were found among these springs in term of hydrodynamics [61]. Until now, little work has been published to demonstrate the different hydrogeological functions of these neighboring springs. This study is to provide a conceptual model of Jinan karst groundwater system by four neighboring springs combined the spring water level data and hydrochemical and isotopic data, and put forward the standpoint that neighboring karst springs with same geological conditions can show different hydrogeological characteristics, which is a useful evidence for understanding the heterogeneity/complexity of karst aquifers. The main objective of this paper is to: (1) reveal the recharge sources of karst springs; (2) identify the hydrogeochemical processes of karst springs; and (3) make clear the hydrodynamic characteristic of karst springs.

2. Study Area

The Jinan karst system extends between the longitudes of 116°11' to 117°44' E and the latitudes of 36°01' to 37°32' N, in the north limb of Mountain Tai anticline with gradually lowering elevation from south to north, characterized by mountainous area in the southern part, inclined piedmont plain in the central part, and alluvial plain in the northern part (Figure 1).

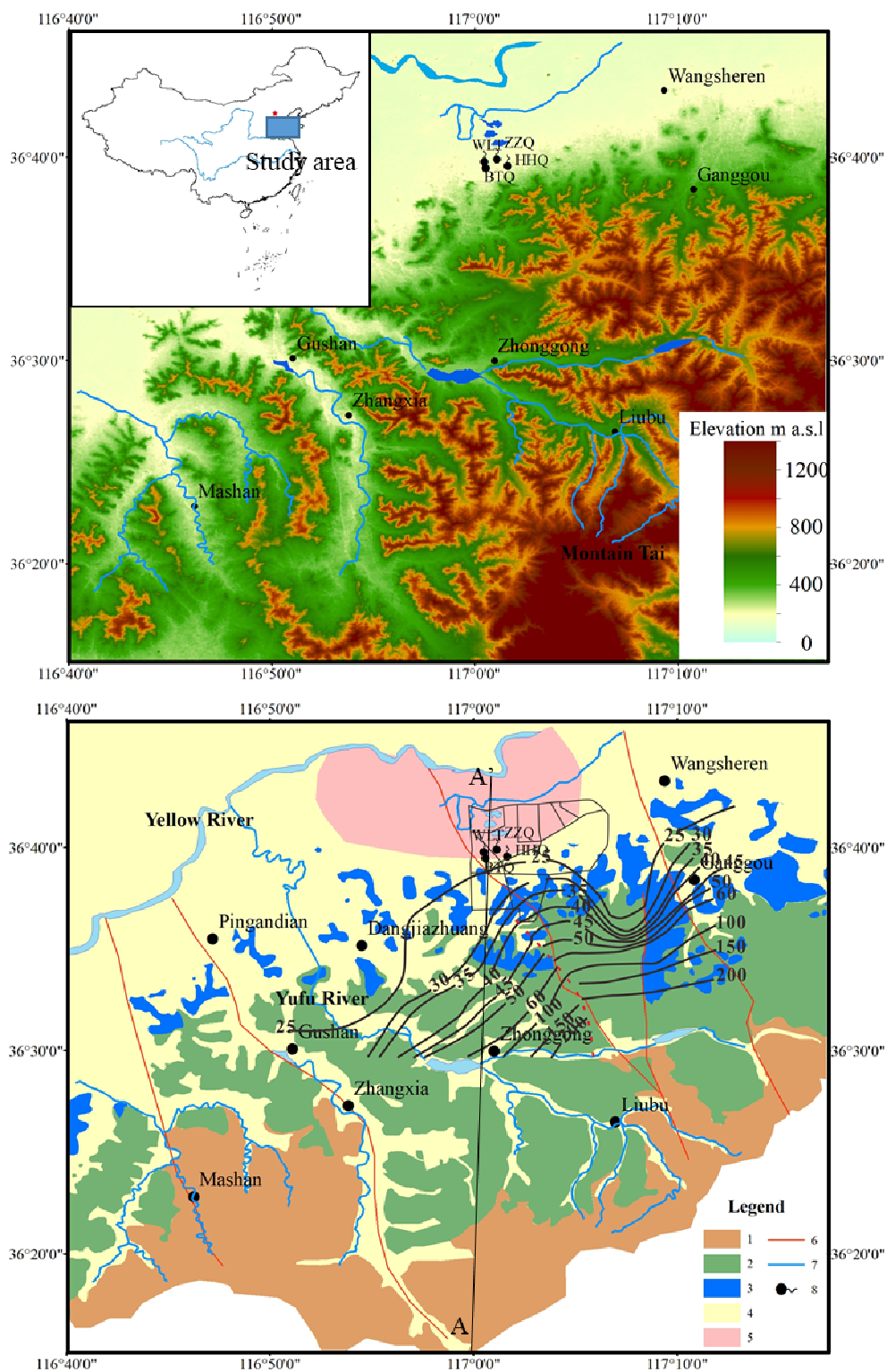


Figure 1. Topographic and generalized geological map in the Jinan karst spring system. (1. Archaean metamorphic rocks; 2. Cambrian limestone; 3. Ordovician limestone; 4. Quaternary sediments; 5. Magmatic rocks; 6. Fault; 7. River; and 8. Spring. The numbers in figure represent the groundwater level obtained from Sun [58] and they show a high hydraulic gradient in direction of southwest for Baotu Spring and southeast for Heihu Spring.)

The climate of Jinan is semiarid continental monsoon climate characterized by cold and dry winter and hot and wet summer. The mean precipitation is 673 mm/year, and around 75% occurs from June

to September. Evaporation rate is 2387 mm/year. Air temperature ranges from $-1.4\text{ }^{\circ}\text{C}$ in January to $27.4\text{ }^{\circ}\text{C}$ in July, with mean temperature of $14.3\text{ }^{\circ}\text{C}$.

Archaean metamorphic rocks are basement and outcrop in the south of the catchment, and northwards, which is overlain by Cambrian and Ordovician carbonate rocks. The limestones and dolomites are massive and well jointed with a stratigraphic thickness of 1300–1400 m. Cambrian strata are composed of thick-bedded limestone, argillaceous limestone, and dolomite limestone, and Ordovician strata are characterized by the inter-bed of limestone and shale. They dip away from the metamorphic rocks at angles varying from 5° to 10° in the dip direction of NW20°. Intrusive magmatic rocks (diorite and gabbro) of Yanshan epoch in Mesozoic are located in the top of Ordovician strata in the north, and the intrusive rocks are buried mostly by Quaternary sediments (Figure 1).

Jinan karst system is an open fracture karst system, consisting of Cambrian and Ordovician carbonate rocks. Precipitation is the main recharge source, and when total precipitation amount within 10 days is greater than 18 mm, the spring water level would respond within 5 days [58]. Yufu River is another recharge source of the karst aquifer [10,62,63]. In dry season, the Yufu River is charged by water drained down from its upstream reservoirs, or transported from Yellow River or Yangtze River through the canal built by the South-to-North Water Diversion Project. The volume of transported water was $43,470,000\text{ m}^3$ in 2015, $34,130,000\text{ m}^3$ in 2016 and $302,400,004\text{ m}^3$ in 2017 (data is obtained from the website (<http://www.whssk.com>)).

The hydraulic conductivity for Jinan karst aquifer ranges from 0.05 m/day to 120 m/day. Groundwater is tending to move from the south toward the north (similar to the dip direction of strata) and is hindered by the intrusive rocks to form discharge areas (Figure 2). In the city of Jinan, 108 karst springs occurred in an area of 2.6 km^2 , with discharge in the range from 3×10^5 to $4 \times 10^5\text{ m}^3/\text{day}$ under natural conditions [57]. These springs emerge in a close spatial area, of which Baotu Spring (BTQ), Heihu Spring (HHQ), Zhenzhu Spring (ZZQ), and Wulong Springs (WLQ) are most well-known. In the location of the BTQ and HHQ, igneous rock thickness is zero, Quaternary sediments connect directly with carbonate rock, and the karst groundwater directly discharge. WLT and ZZQ are mainly from the Cambrian formation with deeper runoff depth, the karst groundwater discharges through igneous rock fractures and exposed surface [62,63]. Origins of BTQ and HHQ are different, BTQ is from west and south, water in HHQ origins from south east by water level monitor [61,64].

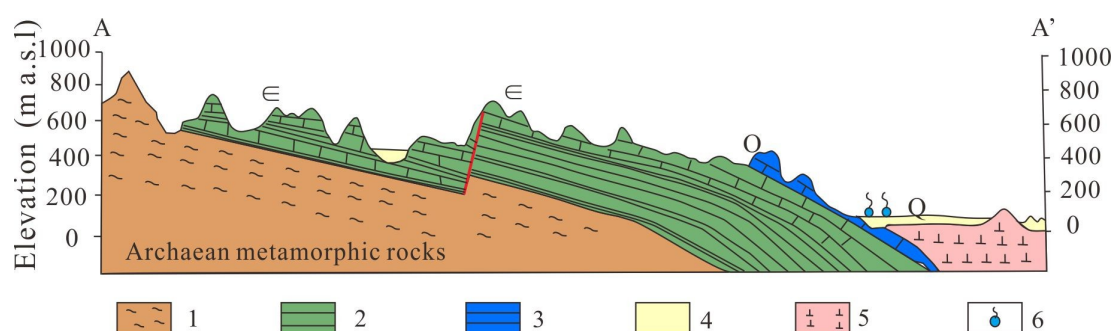


Figure 2. The geological cross map of the Jinan karst spring system. (1. Archaean metamorphic rocks; 2. Cambrian limestone; 3. Ordovician limestone; 4. Quaternary sediments; 5. Magmatic rocks; and 6. Spring).

The total discharge of springs was in the range from 3×10^5 to $4 \times 10^5\text{ m}^3/\text{day}$ in the 1960s, with the maximum value of $5 \times 10^5\text{ m}^3/\text{day}$ in 1962. The average Baotu Spring discharge and Heihu Spring discharge were $7.83 \times 10^4\text{ m}^3/\text{day}$ and $1.12 \times 10^5\text{ m}^3/\text{day}$ for 1959–1972, respectively. With the development of industry and agriculture, groundwater exploitation increased from $7.28 \times 10^4\text{ m}^3/\text{day}$ in 1959 to $5 \times 10^5\text{ m}^3/\text{day}$ in 1981 to $7.689 \times 10^5\text{ m}^3/\text{day}$ in 1993, among which more than 70% was from karst groundwater. The karst springs stopped flowing at the first time in 1972 for the sake of

over exploitation of karst groundwater, and later on, zero flow occurred in 1982, 1989, and 2000–2002. In order to restore the flow of the main springs for environment and tourism, municipal water supply wells were switched off and river water has been used as drinking water, and the main springs have been restored to flow since September 2003.

Figure 3 shows the water level variation of BTQ and HHQ during May 2012 and December 2018 and the precipitation from May 2012 to May 2014. The spring water level shows seasonal fluctuation in response to precipitation with the highest water levels in September and lowest water levels in July. The lag time of spring water level and precipitation is 45 day for 2008–2012 and 90 day for 2006–2008 [65]. The lag time of spring water level and precipitation on year scale for 1959–2011 is around 3–4 months based on wavelet transform [59].

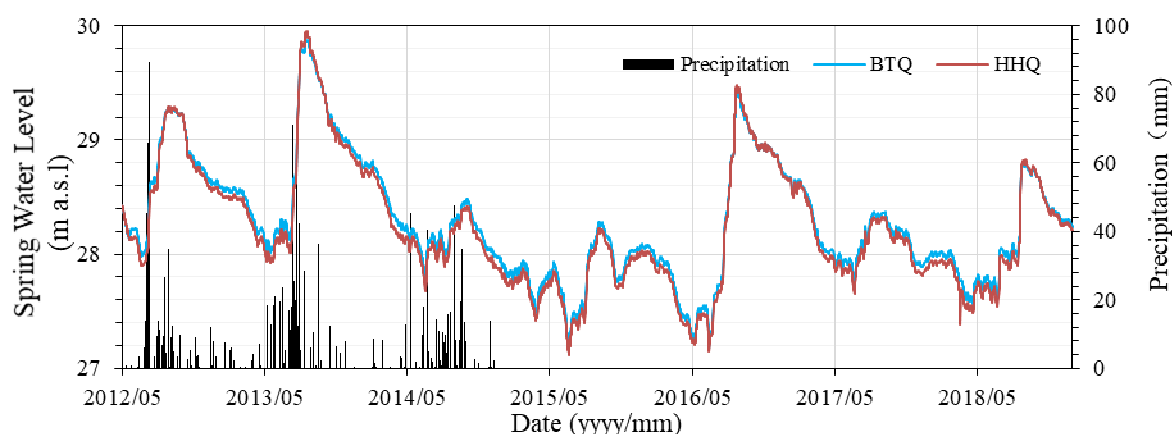


Figure 3. Plots of monthly precipitation and the daily water level of Baotu Spring (BTQ) and Heihu Spring (HHQ).

3. Materials and Methods

This study is based on water sample analyses (hydrogeochemical analyses and stable isotope analyses) together with daily spring water level monitoring. Fifty-six water samples were collected at approximately monthly intervals between May 2015 to October 2016 from BTQ ($n = 13$), HHQ ($n = 13$), WLT ($n = 12$) and ZZQ ($n = 12$), in addition, 4 rainwater samples, and 2 river water samples in Yufu River were collected.

The water samples for cation analysis were collected in high density polyethylene bottles (pre-cleaned with 5% HNO_3 and deionized water), filtered through a $0.45 \mu\text{m}$ membrane filter after sampling, and stabilized by adding 1% HNO_3 immediately after filtration. The samples for anion and stable isotope analysis were collected in 100 mL pre-cleaned glass bottles.

Water temperature, pH, and electrical conductivity (EC) were measured in the situ using portable multi-parameter instrument (Multi 340i/SET) (WTW a xylem brand, Weilheim, Germany), with the precision of $\pm 0.1 \text{ }^\circ\text{C}$ for temperature and $\pm 1 \mu\text{s/cm}$ for EC.

Bicarbonate (HCO_3^-) was titrated with 0.05 M HCl. The major anions (Cl^- , SO_4^{2-} and NO_3^-) and cations (K^+ , Na^+ , Ca^{2+} and Mg^{2+}) were measured using Dionex DX-120 Ion Chromatography (Thermo Fisher Scientific, Washington, DC, USA). Based on the reproducibility for replicate samples, the analytical precision for ion analysis is $\pm 5\%$. Water stable isotopes ($^2\text{H}/\text{H}$ and $^{18}\text{O}/\text{O}$) were measured using the Finnigan MAT 253 mass spectrometer (Scientific Instrument Services, INC, New Jersey, NJ, USA). The results are reported in $\delta\text{‰}$ referred to VSMOW (Vienna Standard Mean Ocean Water). The measurement precision for $\delta^2\text{H}$ and $\delta^{18}\text{O}$ is $\pm 1.0\text{‰}$ and $\pm 0.2\text{‰}$, respectively. All chemical and isotopic analyses were performed at the Institute of Geology and Geophysics of the Chinese Academy of Sciences (IGG-CAS).

The saturation index for calcite (SIc), dolomite (SI_d) and gypsum (SI_g) in water samples and the water type were calculated by the software of AquaChem (3.7) and PHREEQC [66], respectively.

In addition, the daily water level of BTQ and HHQ from 2 May 2012 and 31 December 2018 were obtained, with 2427 sets of water level data from Jinan water conservancy bureau (<http://www.jnwater.gov.cn/>). The date precipitation information of 2013 and 2014 is obtained from Shandong Province weather bureau.

4. Results

4.1. Hydrogeochemistry

The water temperature ranged from 16.9 °C to 23.4 °C for BTQ, from 16.6 °C to 18.3 °C for HHQ, from 17.5 °C to 19 °C for WLT, and from 16.4 °C to 21.6 °C for ZZQ. There were peaks in temperature series in BTQ and ZZQ on 19 June (Figure 4). The pH value in spring water ranged from 7.20 to 7.48 for BTQ, from 7.18 to 7.49 for HHQ, from 7.27 to 7.56 for WLT, and from 7.27 to 7.97 for ZZQ. In terms of pH series, there were valleys on 7 August for all the four springs, and there was a peak in ZZQ on 19 June, and a valley in HHQ on 19 June (Figure 4). The electrical conductivity (EC) in spring water ranged from 753 $\mu\text{s}/\text{cm}$ to 872 $\mu\text{s}/\text{cm}$ for BTQ, from 814 $\mu\text{s}/\text{cm}$ to 901 $\mu\text{s}/\text{cm}$ for HHQ, from 665 $\mu\text{s}/\text{cm}$ to 784 $\mu\text{s}/\text{cm}$ for WLT, and from 655 $\mu\text{s}/\text{cm}$ to 995 $\mu\text{s}/\text{cm}$ for ZZQ. The EC values in HHQ did not show fluctuation, while there a peak in the EC series in BTQ, WLT, and ZZQ on 19 June (Figure 4).

The spring water was characterized by low level of mineralization with TDS (total dissolved solutions) between 321.7 mg/L and 530.4 mg/L. The springs can be listed by HHQ > BTQ > WLT > ZZQ in descending order based on the TDS in the spring water. Table 1 shows the statistic information about major ion concentration in the water samples collected from BTQ, HHQ, WLT, and ZZQ. For all the four karst springs, HCO_3^- and SO_4^{2-} were the dominant anions, Ca^{2+} was the dominated cation.

The concentration of HCO_3^- ranged from 241.7 mg/L to 307.2 mg/L for BTQ, from 282.4 mg/L to 316.2 mg/L for HHQ, from 223.4 mg/L to 333.2 mg/L for WLT, and from 213.6 mg/L to 279.1 mg/L for ZZQ. There were valleys in the time series of HCO_3^- concentration on 19 June in BTQ, WLT, and ZZQ, while this concentration valley did not show in HHQ (Figure 4).

The concentration of Ca^{2+} varied from 63.3 mg/L to 103.3 mg/L for BTQ, from 83.7 mg/L to 116.1 mg/L for HHQ, from 57.8 mg/L to 84.3 mg/L for WLT, and from 50.1 mg/L to 88.63 mg/L for ZZQ. The Ca^{2+} concentration showed similar temporal fluctuation with HCO_3^- concentration, with valleys in BTQ, WLT, and ZZQ on 19 June, which did not show in HHQ (Figure 4).

The concentration of SO_4^{2-} ranged from 70.4 mg/L to 105.9 mg/L for BTQ, from 80.7 mg/L to 107.7 mg/L for HHQ, from 58.8 mg/L to 84.1 mg/L for WLT, and from 61.1 mg/L to 144.1 mg/L for ZZQ. The temporal variation of SO_4^{2-} concentration in the spring water was opposite with HCO_3^- concentration and Ca^{2+} concentration. There were peaks in the SO_4^{2-} concentration series in BTQ, WLT, and ZZQ on 19 June, which did not show in HHQ. The concentration peaks in series of Cl^- and Na^+ on 19 June were more, which also did not show in HHQ. The NO_3^- concentration ranged between 18.23 mg/L and 44.58 mg/L (averagely 34.7 mg/L) in BTQ, and between 30.47 mg/L and 57.50 mg/L (averagely 40.3 mg/L) in HHQ.

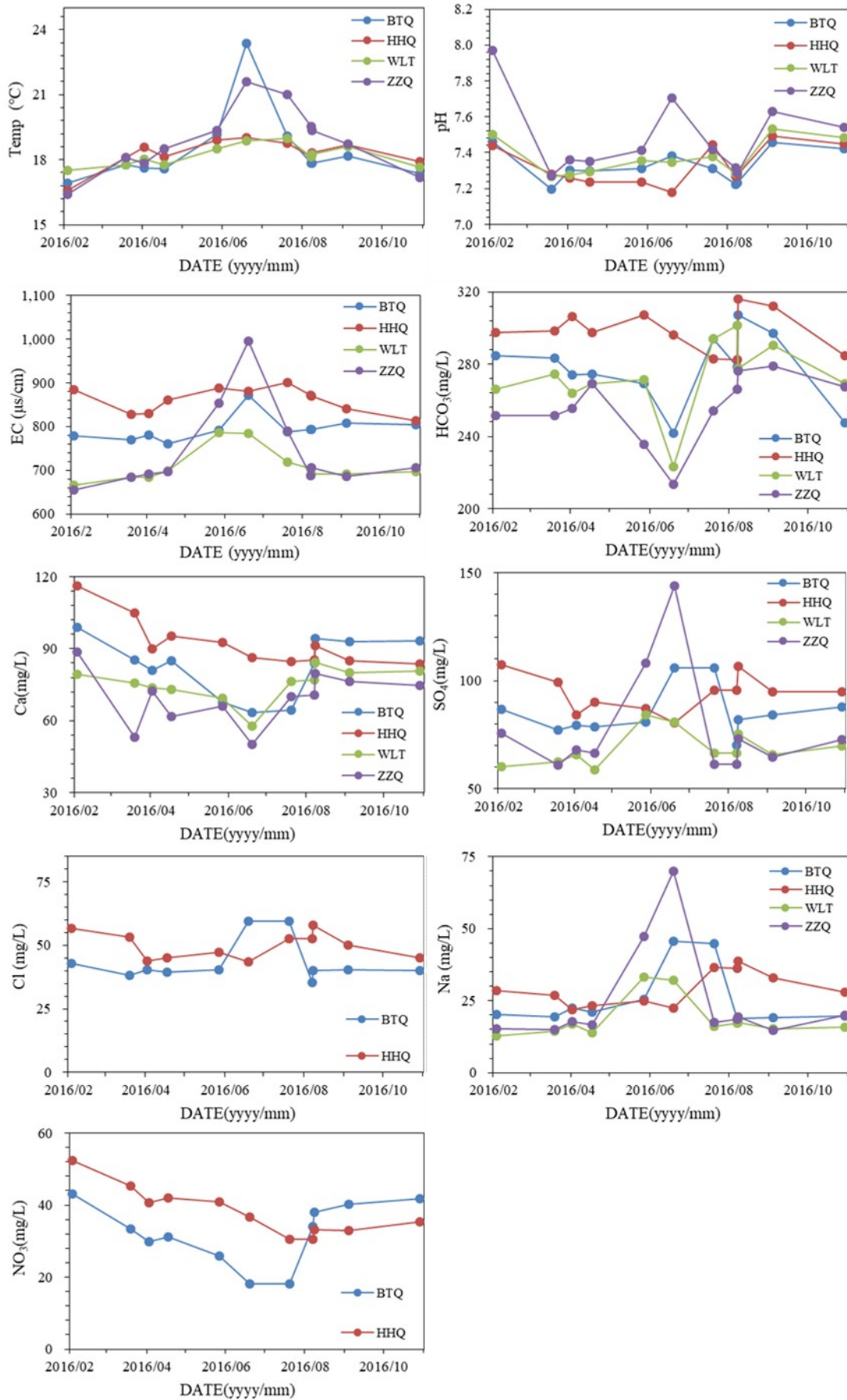


Figure 4. The temporal series of physical and chemical parameters in karst springs.

Table 1. The statistic values of major ion components in spring water, river water, and rain water.

Spring		EC	HCO ₃ ⁻	SO ₄ ²⁻	NO ₃ ⁻	Cl ⁻	Ca ²⁺	Mg ²⁺	Na ⁺	K ⁺	δ ¹⁸ O	δ ² H
BTQ n = 13	Max	872.0	307.2	105.9	44.6	59.4	101.3	17.6	45.7	2.7	-8.17	-59.36
	Min	753.0	241.7	70.4	18.2	34.5	63.3	13.3	16.3	0.9	-8.75	-61.33
	Mean	788.2	276.7	84.4	33.4	42.5	83.8	15.8	24.0	1.3	-8.41	-60.19
	St.D	29.4	17.4	10.4	8.3	7.5	12.2	1.1	9.3	0.6	0.17	0.65
	C.V	4.0	6.0	12.0	25.0	18.0	15.0	7.0	39.0	46.0	1.98	1.08
HHQ n = 13	Max	901.0	316.2	107.7	57.5	57.8	116.1	19.6	38.8	1.8	-7.93	-55.76
	Min	814.0	282.4	80.7	30.5	39.7	83.7	14.8	21.7	0.9	-8.61	-61.06
	Mean	860.5	297.1	94.5	40.3	49.0	93.7	16.6	28.5	1.2	-8.29	-59.12
	St.D	3.0	4.0	9.0	20.0	11.0	11.0	7.0	20.0	29.0	0.19	1.39
	C.V	0.0	0.0	0.1	0.2	0.1	0.1	0.1	0.2	0.3	2.27	2.35
WLT n = 12	Max	786.0	333.2	84.1	38.8	45.9	84.3	15.9	33.1	1.3	-8.11	-58.17
	Min	665.0	223.4	58.8	23.7	22.0	57.8	13.2	12.8	0.7	-8.99	-62.51
	Mean	709.3	277.9	69.1	28.9	31.5	74.0	14.6	19.1	1.0	-8.43	-60.25
	St.D	37.9	25.1	7.6	3.8	6.2	7.6	0.8	6.6	0.2	0.21	0.98
	C.V	5.0	9.0	11.0	13.0	20.0	10.0	5.0	35.0	20.0	2.45	1.63
ZZQ n = 12	Max	995.0	279.1	144.1	36.9	82.4	88.6	19.8	70.0	2.3	-7.66	-57.03
	Min	655.0	213.6	61.1	13.7	25.5	50.1	13.7	14.8	0.9	-8.66	-61.06
	Mean	740.7	255.2	76.9	26.2	36.6	69.2	15.2	24.3	1.3	-8.20	-59.26
	St.D	96.7	17.8	23.6	5.6	16.1	10.3	1.7	16.1	0.4	0.25	1.09
	C.V	13.0	7.0	31.0	21.0	44.0	15.0	11.0	66.0	30.0	3.04	1.84
YF	Mean	549	112.9	134.3	8.7	38.4	51.1	18.0	25.3	2.75	-6.0	-10.7
Rain	Mean	-	39.5	2.7	1.9	6.7	0.25	2.3	3.0	3.5	-46.4	-73.7

Note: BTS: Baotu Spring; HHS: Heihu Spring; Rain: rain water; YF: the water from Yufu River; the unit of electrical conductivity is $\mu\text{S}/\text{cm}$, and the unit of ion concentration is mg/L .

Saturation index (SI) quantitatively describes the deviation of water from equilibrium with respect to the dissolved mineral [67]. The calcite saturation index (SI_c) ranged from -0.09 to 0.25 for water from BTQ, from -0.18 to 0.28 for water from HHQ, from -0.17 to 0.27 for water from WLT, and from -0.23 to 0.67 for water from ZZQ, indicating the spring water was generally saturated with calcite. The saturation index of dolomite (SI_d) ranged from -1.04 to -0.02 for water from BTQ, and from -0.92 to 0.08 for water HHQ, from -0.67 to 0.07 for water from WLT, and from -0.79 to 0.84 for water from ZZQ, indicating the spring water was unsaturated with dolomite. The variation of gypsum saturation index (SI_g) was limited, from -1.72 to -1.56 for water from BTQ, from -1.64 to -1.44 for water from HHQ, from -1.81 to -1.67 for water from WLT, and from -1.91 to -1.62 for water from ZZQ, indicating the spring water was unsaturated with gypsum.

The water type of spring water samples were mostly Ca-HCO₃-SO₄ (Figure 5), two samples from BTQ, three sample from HHQ, two sample from WLT and one sample from ZZQ had water type of Ca-Na-HCO₃-SO₄, one sample from WLT had water type of Ca-HCO₃, and one sample from ZZQ had water type of Na-Ca-HCO₃-SO₄. Compared with spring water, water from Yufu River had higher concentration of SO₄²⁻, Cl⁻, Na⁺, Mg²⁺, and K⁺, and lower concentration of HCO₃⁻, NO₃⁻, and Ca²⁺ with the water type of Ca-SO₄.

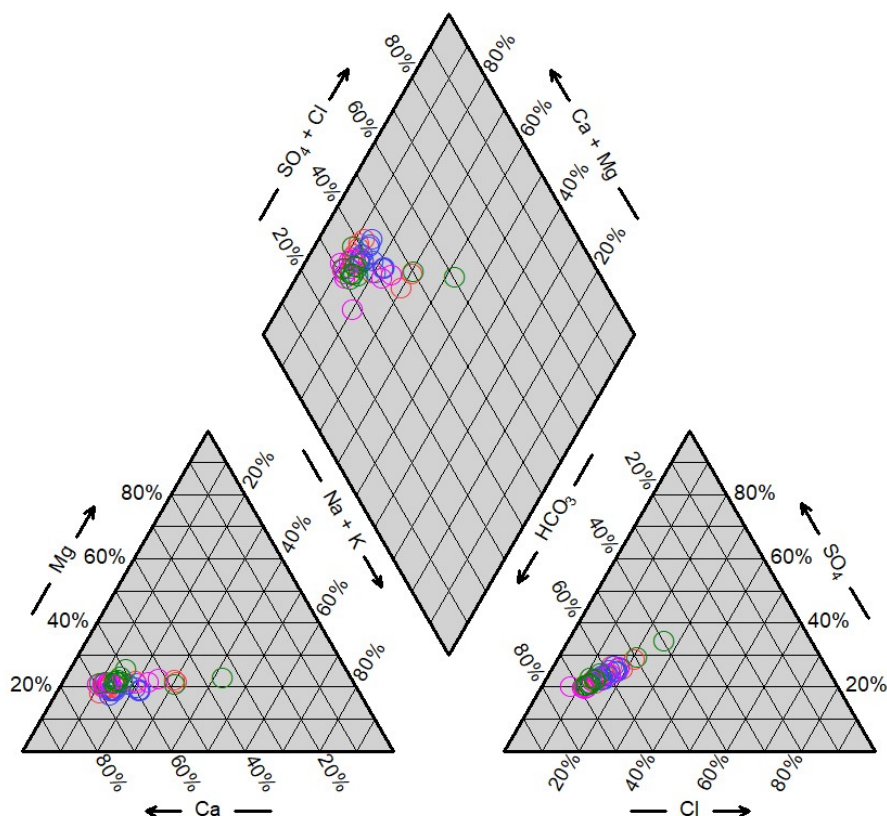


Figure 5. The Piper Diagram of spring water samples. (The red circle is for Baotu Spring, the blue circle is for Heihu Spring, the violet circle is for Wulong Spring, and the green circle is for Zhenzhu Spring).

4.2. Stable Isotopes

The $\delta^2\text{H}$ and $\delta^{18}\text{O}$ values of the four rain samples were the most depleted among water samples, ranging from -86.80‰ to -62.17‰ and -12.28‰ to -9.25‰ , respectively. The $\delta^2\text{H}$ and $\delta^{18}\text{O}$ in the Yufu River were the most enriched, ranging from -46.8‰ to -45.9‰ and from -6.11‰ to -5.9‰ , respectively. The $\delta^{18}\text{O}$ and $\delta^2\text{H}$ values ranged from -8.75‰ to -8.17‰ , and -61.33‰ to -59.36‰ for BTQ, from -8.61‰ to -7.93‰ , and -61.06‰ to -55.76‰ for HHQ, from -8.99‰ to -8.11‰ , and -62.51‰ to -58.17‰ for WLT, and from -8.66‰ to -7.66‰ , and -61.06‰ to -57.03‰ for ZZQ, respectively.

The spring water samples lie below the global meteoric water line (GMWL: $\delta^2\text{H} = 8\delta^{18}\text{O} + 10$, [68]). The local meteoric water line (LMWL) was obtained from the rain water samples as $\delta^2\text{H} = 8.26\delta^{18}\text{O} + 13.38$, (0.9995) (Figure 6). The regression lines of stable isotope values in BTQ, HHQ, WLT, and ZZQ based on least square method are $\delta^2\text{H} = 3.5\delta^{18}\text{O} - 31.0$ ($R^2 = 0.78$), $\delta^2\text{H} = 6.7\delta^{18}\text{O} - 3.6$ ($R^2 = 0.8$), $\delta^2\text{H} = 3.8\delta^{18}\text{O} - 28.0$ ($R^2 = 0.65$), and $\delta^2\text{H} = 3.8\delta^{18}\text{O} - 28.3$ ($R^2 = 0.74$), respectively. The low slopes of the relationship line for BTQ (3.5), WLT (3.8) and ZZQ (3.8) indicate the spring water is mixing with other water and/or undergoes an evaporative process.

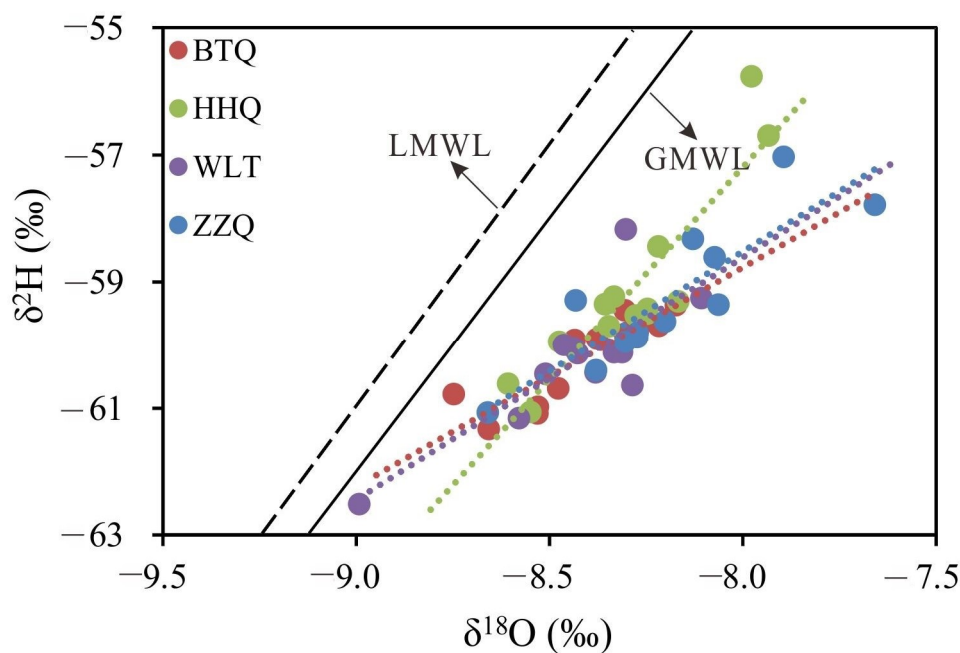


Figure 6. The relationship of $\delta^{18}\text{O}$ and $\delta^2\text{H}$ in spring samples from BTQ, HHQ, WLT, and ZZQ.

5. Discussion

BTQ, HHQ, WLT, and ZZQ closely located with same geological background, while the four karst springs have different hydrogeochemical and isotopic characteristics although they are located in close proximity. Based on hydrogeological conditions and above results, BTQ, WLT, and ZZQ have similar behaviors, which are different with that of HHQ. In the following discussion, BTQ and HHQ are compared to characterize the Jinan karst aquifer.

5.1. Recharge Sources

The minimum value of HCO_3^- concentration in BTQ and HHQ occurs on a different date in 2016. The minimum value of HCO_3^- concentration in BTQ is 241.7 mg/L, occurs on 19 June, while the minimum value of HCO_3^- concentration in HHQ is 282.4 mg/L, and occurs on 7 August.

The minimum value of HCO_3^- concentration in HHQ is the result of dilution of rain water as there was a heavy rainfall event on 7 August. The rain water diluted the concentration of HCO_3^- , Ca^{2+} , SO_4^{2-} , Cl^- , Na^+ , and NO_3^- both in BTQ and HHQ, and the ion concentration increased one day after the rainfall event. One day after the rainfall event, the TDS increased from 377.3 mg/L to 421.3 mg/L and from 427.8 mg/L and 459.5 mg/L, the saturation index of calcite increased from -0.06 to 0.02 and from -0.02 to 0.07 , the saturation index of dolomite increased from -0.62 to -0.46 and from -0.48 to -0.33 , the saturation index of gypsum increased from -1.7 to -1.61 and from -1.58 to -1.52 for water from BTQ and HHQ, respectively. The above results show the springs mainly discharge the storage water as the storage water has enough residence time to share higher TDS and saturation index.

Once the differences in $\delta^{18}\text{O}$ of rain water—spring water before the rainfall event and spring water after rainfall event have been established—the simple isotope binary mixture model can be used to calculate the contribution of rainwater for spring discharge. The $\delta^{18}\text{O}$ value for rain water in 7 August is -12.1‰ , the $\delta^{18}\text{O}$ value decreases from -8.43‰ to -8.75‰ and from -7.98‰ to -8.22‰ for samples collected on 7 August and 8 August for BTQ and HHQ, respectively. Therefore, the proportion of rain water in BTQ and HHQ one day after rainfall event is 5.8% and 8.5%, respectively. This result again illustrates the springs mainly discharge the storage water in aquifer one day after rainfall event.

While the minimum value of HCO_3^- concentration in BTQ occurred on 19 June, there is no rain around that day from local weather record. Therefore, there must be other recharge sources for the least HCO_3^- concentration in BTQ, which do not influence the HHQ. This kind of recharge source

also decrease the concentration of Ca^{2+} and NO_3^- . In addition, the maximum value of concentration for SO_4^{2-} , Cl^- , and Na^+ in BTQ also occur on 19 June, and no concentration peak exhibits on HHQ on that day. Considering river water has higher concentration of SO_4^{2-} , Cl^- , and Na^+ , and lower concentration of HCO_3^- , Ca^{2+} , and NO_3^- compared with that in spring water. Therefore, river water recharge is an important recharge source for BTQ, which does not show influence on HHQ.

The regression line of stable isotope in HHQ ($\delta^2\text{H} = 6.7\delta^{18}\text{O} - 3.6$ ($R^2 = 0.8$)) is nearly parallel with LMWL, indicating the spring water mainly originates the direct infiltration of rain water. While the regression line of stable isotope in BTQ ($\delta^2\text{H} = 3.5\delta^{18}\text{O} - 31.0$ ($R^2 = 0.78$)) has less slope, indicating there are other recharge origins with enriched stable isotope value except precipitation. River water is an important recharge for the Jinan karst aquifer [10,63]. The average $\delta^{18}\text{O}$ value of river water is 6.0‰, which is more enriched than that of spring water. After infiltration into the underground, the river water would increase the $\delta^{18}\text{O}$ value of groundwater and decrease the slope of regression line of stable isotope.

The $\delta^{18}\text{O}$ values in HHQ show seasonal variation with depleted values in the dry season and enriched values in the wet season (Figure 7). In comparison, the $\delta^{18}\text{O}$ values in BTQ show irregular variation, generally, with enriched values in dry season and depleted values in wet season. It is that the $\delta^{18}\text{O}$ value for the sample collected in BTQ on 19 June is higher than the sample collected in other date. Therefore, water from the Yufu River is an important recharge source for the Baotu Spring in the dry season.

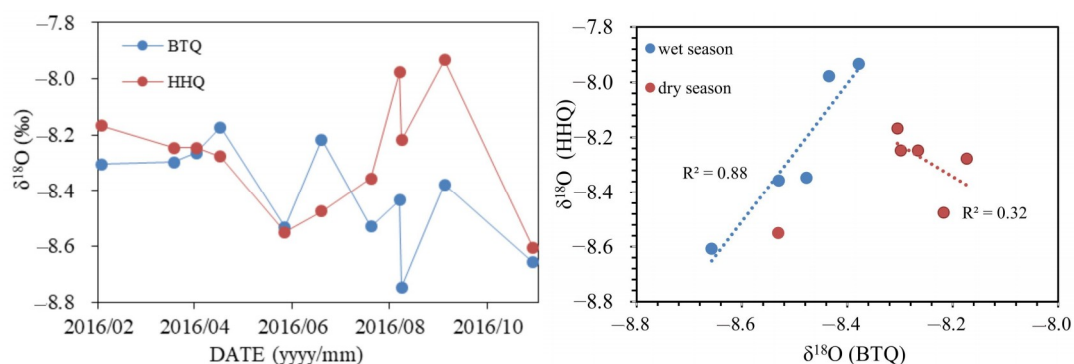


Figure 7. The temporal variation of $\delta^{18}\text{O}$ values in springs and the relationship of $\delta^{18}\text{O}$ values in BTQ and HHQ.

However, the river water does not influence HHQ, as HHQ does not show hydrogeochemical and stable isotopic response. In addition, the relationship of $\delta^{18}\text{O}$ values between the samples from BTQ and HHQ is positive for samples collected in the wet season with a correlation coefficient of 0.88, while negative for samples collected in the dry season with a correlation coefficient of 0.32 except one couple of samples (This couple samples were collected on 27 May, when there was a rainfall). All in all, the different temporal variation of hydrogeochemistry and stable isotope in BTQ and HHQ prove these two springs have different recharge sources, which is mainly the precipitation for HHQ and the precipitation and river water for BTQ.

5.2. Hydrogeochemical Processes

The saturation index of calcite (Sic) and dolomite (Sid) in spring water have relation with water level (Figure 8). For BTQ, Sic, and Sid have no relation with water level during low water level period, and positive with water level during high water level period. For HHQ, Sic, and Sid are positive with water levels in both the low and high spring water level period. Simultaneous consideration of hydrogeochemistry and spring discharge could reveal the hydrogeochemical processes in aquifers [2,47,51]. The strong relationship between hydrogeochemistry and spring water level proves there is a functional relationship between the water level and hydrogeochemistry.

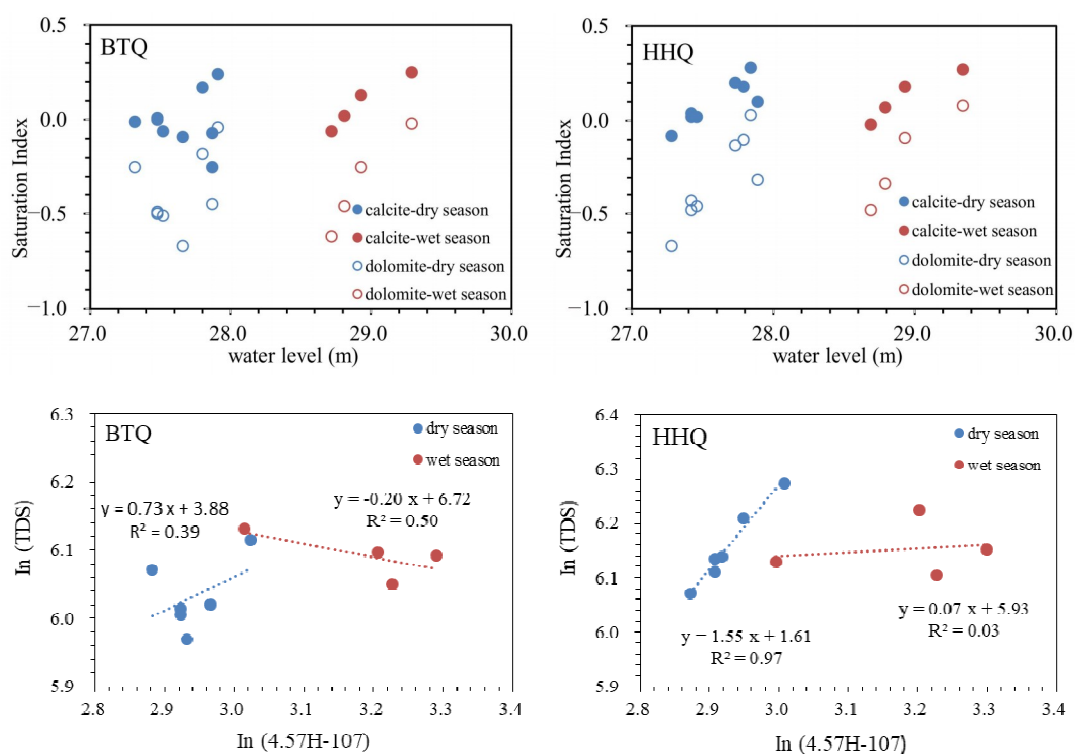


Figure 8. The relationship between water level and saturation index of calcite and dolomite and the relationship between and water level with TDS (total dissolved solutions) in BTQ and HHQ.

In order to quantify the relationship between spring water level and ion concentration, the equation is modified on the basis of the Function (1) from Grasso [69] and the Function (2) from Kang [57].

$$C = A \times e^{-\alpha \times \ln(Q)} \quad (1)$$

$$Q = 4.57 \times H - 107 \quad (2)$$

Q is spring discharge ($10^4 \text{ m}^3/\text{day}$) and H is the spring water level elevation (m a.s.l.).

This exponential function can be expressed as the pair of C(t)/H(t) presented on a logarithmic plot fall on a straight line as:

$$\ln(C) = A + \alpha \times \ln(4.57 \times H - 107) \quad (3)$$

α : a parameter reflects the relative importance of dilution and dissolution;

A: a constant.

Depending on the α value, three cases can be identified:

$\alpha = 0$ the ion concentration is stable;

$\alpha > 0$ the ion concentration rises with an increasing spring water level, indicating dissolution is more important as the mass flux is more than that the volumetric flux;

$\alpha < 0$ the concentration declines with an increasing spring water level, indicating dilution is more important as volumetric flux is more than that of the dissolved mass flux.

The two springs show different relationships between water level and TDS, reflecting different hydrogeochemical processes for these two springs. In the dry season, both BTQ and HHQ have a positive α value, indicating dissolution is the major hydrogeochemical process. In the wet season, the value of α in BTQ is negative, indicating dilution is the major hydrogeochemical process, while the value of α in HHQ is nearly zero, indicating the stable ion concentration.

The HCO_3/Ca ratio ranges from 1.74 to 3 with an average value of 2.21 for BTQ, and from 1.68 to 2.41 with an average value of 2.1 for HHQ, indicating the dissolution process is mainly controlled by

calcite and dolomite. Same result could also be obtained by the Mg/Ca ratio, which ranges from 0.26 to 0.46 with an average value of 0.32 for BTQ and varies from 0.25 to 0.34 with an average of 0.3 for HHQ.

The HCO_3^-/Ca ratio in BTQ is higher than that in HHQ from February to July, and less than that in HHQ from August to November, similar behavior also occurs for Mg/Ca ratio (Figure 9), indicating the different seasonal hydrogeochemical processes. For BTQ, the HCO_3^-/Ca ratio and Mg/Ca ratio are higher from May to July, indicating more dolomite dissolution in this period. While for HHQ, the HCO_3^-/Ca ratio and Mg/Ca ratio are higher from August to November, indicating more dolomite dissolution from August to November.

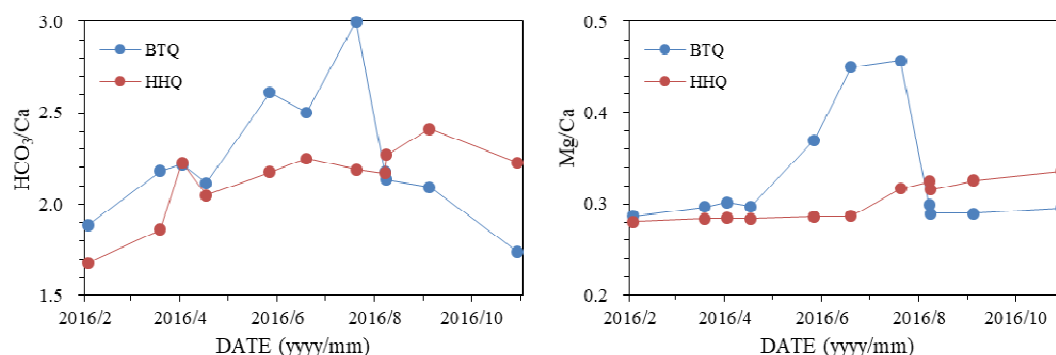


Figure 9. The temporal variation of HCO_3^-/Ca and Mg/Ca in BTQ and HHQ.

Except mineral dissolution, the two springs also show different responses to human activities. The NO_3^- of BTQ and HHQ show a similar decreasing trend in the dry season, while the NO_3^- of BTQ increases more than that of HHQ in the wet season. In the wet season, the rain water would carry the NO_3^- into aquifer from soil layer, increases the NO_3^- in karst groundwater. The higher NO_3^- in BTQ reflects BTQ is more sensitive to agriculture activity. Therefore, BTQ and HHQ not only have different recharge sources, but also experience different hydrogeochemical processes.

5.3. Spring Water Level Hydrodynamic Processes

Limited by the local condition, it is not easy to measure the spring discharge, and there are automatic observation water level gauges that could provide the daily spring water level with a high precision of mm. According to the long term observation of spring discharge and groundwater level in the Jinan spring catchment, there is a strong positive relationship between spring discharge and groundwater level with a coefficient of 0.80 [57].

The water level of BTQ and HHQ have a similar seasonal trend, with the highest water level in September and the lowest water level in July. However, there are also some differences between the water level of BTQ and HHQ. In the years of 2012, 2013, 2016, and 2018, the water level of BTQ is around 5 cm higher than the water level of HHQ in the dry season, while 5–15 cm lower than HHQ in the wet season. Similar spring water level behaviors are also observed in the year of 2010 and 2011, when the water level in BTQ is 3–4 cm higher than the water level in HHQ in the dry season, and 5 cm lower than that of HHQ in the wet season [61]. In the years of 2014, 2015, and 2017, the water level of BTQ is higher than the level of HHQ for both the wet and dry seasons.

The water level difference (ΔH) is defined as the water level of the Baotu Spring minus the water level of the Heihu Spring. From Figure 10, the distribution of the water level difference (ΔH) against the water level of BTQ/HHQ is arc-shaped. The maximum water level difference occurs at the water level of 27.9 m and zero water level difference occurs at water level of 29 m. Given the zero outflow elevation of BTQ and HHQ is 27 m, three conditions are obtained:

1. At the water level between 27 m and 27.9 m, the water level of BTQ is higher than that of HHQ, and the water level difference ($\Delta H > 0$) increases with the spring water level.

- At the water level between 27.9 m and 29 m, the water level of BTQ is also higher than that of HHQ, while the water level difference ($\Delta H > 0$) decreases with the increase of spring water level.
- At the water level higher than 29 m, the water level of BTQ is lower than that of HHQ. At the same time the water level difference ($\Delta H < 0$) increases with the increase of spring water level.

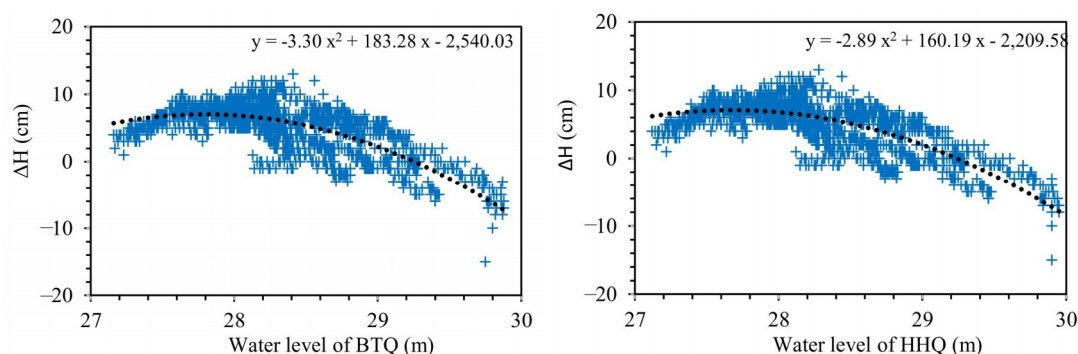


Figure 10. The water level difference between BTQ and HHQ. ($\Delta H = L_{BTQ} - L_{HHQ}$, L_{BTQ} is the water level of BTQ and L_{HHQ} is the water level of HHQ).

The water level differences vary with the spring water level, which illustrates the different water level dynamic of BTQ and HHQ, and reflects the degree of karstified vertical zoning. Two reasons attribute the water level differences between BTQ and HHQ, the different responses to precipitation, and the different depletion processes.

There was a storm on 7 August with total precipitation of 50 mm. Before the storm, from 1 August to 6 August, the water level of both BTQ and HHQ increased at the rate of 4 cm/day. From 7 August to 8 August, water level of BTQ increased at the rate of 9 cm/day, while the water level of HHQ increased at the rate of 11 cm/day. The higher response rate of HHQ than that of BTQ indicates HHQ is more sensitive to precipitation recharge in term of water level, which explains the water level of HHQ exceeding the water level of BTQ in the wet season. For example, in the year 2016, the water level of BTQ was higher than that of HHQ before 11 August, equal with 28.85 m on 11 August, and lower than that of BTQ after that day.

A recession analysis has been done for each spring hydrograph following the method proposed by Birk [70]. Data used in the recession analysis were the spring water level from September to December in the years of 2012–2018 (Figure 11). The depletion coefficient (α) varies each year from $1.57 \times 10^{-3} \text{ day}^{-1}$ to $7.18 \times 10^{-3} \text{ day}^{-1}$ t for BTQ and from $1.56 \times 10^{-3} \text{ day}^{-1}$ t to $7.95 \times 10^{-3} \text{ day}^{-1}$ t for HHQ. The depletion coefficient (α) of HHQ is generally higher than that of Baotu Spring. The higher depletion coefficient for HHQ explains the lower water level of HHQ in the dry season than that of BTQ. Therefore, through analysis the daily spring water level data, BTQ and HHQ have different hydrodynamic characteristics, which may have resulted from inner factor (the heterogeneity of karst conduit/fissure) or outer factor (recharge amount).

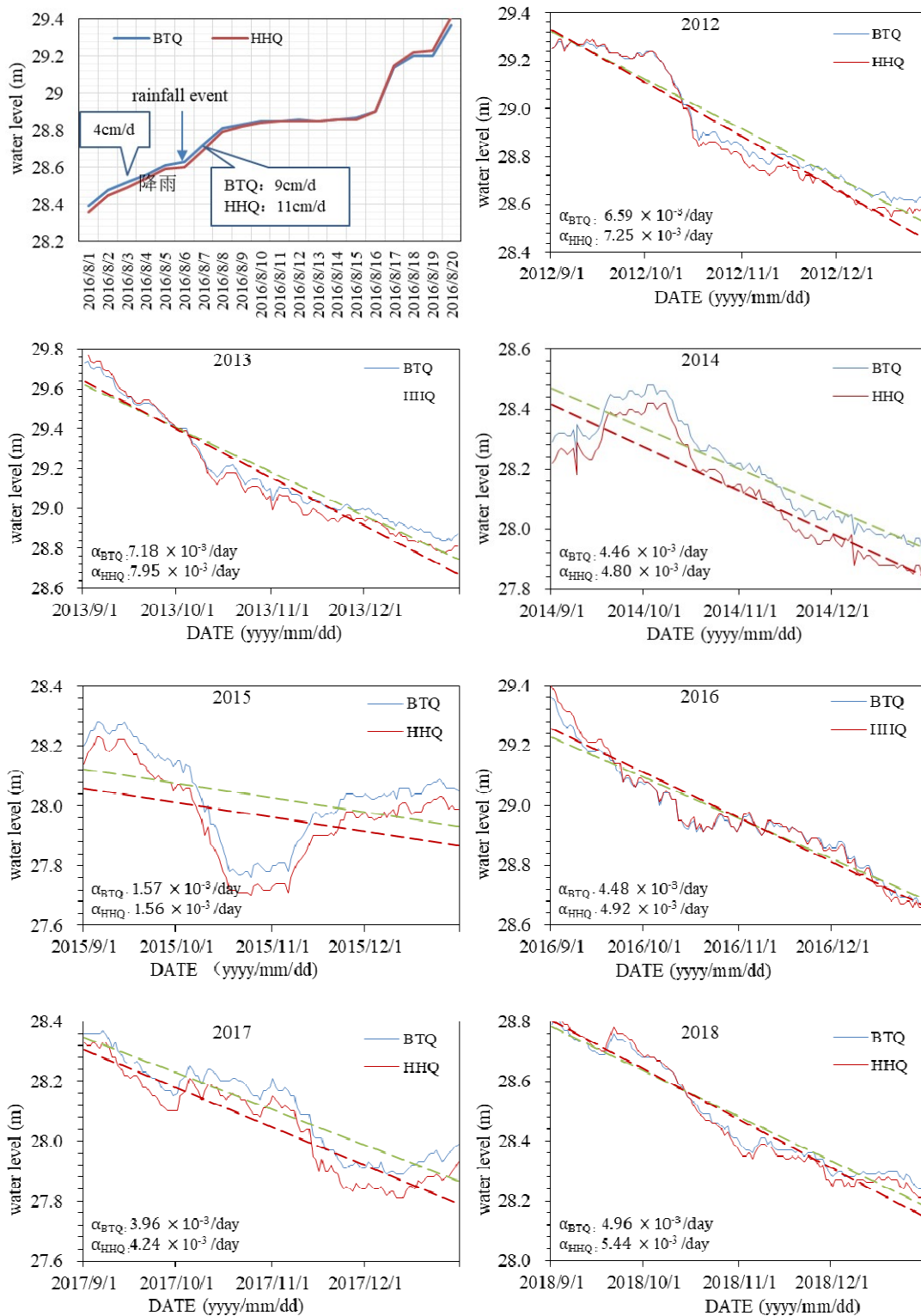


Figure 11. The water level response to rainfall event and the depletion hydrograph in BTQ and HHQ.

6. Conclusions

We detailed the analyses of the water level, hydrogeochemistry, and stable isotope data of two neighboring karst springs, Baotu Spring (BTQ) and Heihu Spring (HHQ), that are within a distance of 430 m, to reveal the different recharge sources, hydrogeochemical processes, and hydrodynamic characteristics. Our results lead to the following conclusions:

1. The different temporal variations of hydrogeochemistry and stable isotope prove BTQ and HHQ have different recharge sources. BTQ is mainly recharged by precipitation and river water, while HHQ is mainly recharged by precipitation.
2. The different relationship between spring water level and hydrogeochemistry reflect the different hydrogeochemical processes of BTQ and HHQ. Based on the ion ratios, the two springs experience different seasonal hydrogeochemical processes, more dolomite dissolution in the dry season and less dolomite dissolution in the wet season in BTQ compared to HHQ. In addition, the different seasonal variations of nitrate show BTQ is more sensitive to agriculture activities than HHQ.
3. The two springs have different hydrodynamic conditions, caused by the vertical zoning of karstification. HHQ responses more quickly to a rainfall event and drains more quickly than BTQ, which results in the water level of BTQ being higher than HHQ in the dry season and lower in the wet season.

All in all, this study highlights the viewpoint that the neighboring karst springs could show different behaviors and belong to different flow systems. The differences between the neighboring karst springs are the evidence that reveals the complexity of the karst system.

Author Contributions: Y.G., D.Q., L.L., and J.S. did the preliminary studies, designed and performed the experiments, conducted field studies, analyzed the data and wrote the paper. F.L and J.H. help the field investigations.

Funding: This research was funded by National Natural Sciences Foundation of China, grant No. 41172215.

Acknowledgments: This study was funded by the National Natural Sciences Foundation (41172215), the project of pilot technology support scheme on aquatic ecological civilization of Water Resources Department of Shandong Province and Shandong Province Financial Bureau. IGGCAS (Institute of Geology and Geophysics, Chinese Academy of Science) is highly acknowledged for managing the grant and facilitating field work. The authors would like to thank Feng Wang for his help on hydrochemical sampling campaigns.

Conflicts of Interest: The authors declare no conflict of interest.

References

1. Ford, D.C.; Williams, P.W. *Karst Hydrogeology and Geomorphology*; John Wiley & Sons: Hoboken, NJ, USA, 2007.
2. Hartmann, A.; Goldscheider, N.; Wagener, T.; Lange, J.; Weiler, M. Karst water resources in a changing world: Review of hydrological modeling approaches. *Rev. Geophys.* **2014**, *52*, 218–242. [[CrossRef](#)]
3. Bakalowicz, M. Karst groundwater: A challenge for new resources. *Hydrogeol. J.* **2005**, *13*, 148–160. [[CrossRef](#)]
4. White, W.B. Karst hydrology recent developments and open questions. *Eng. Geol.* **2002**, *65*, 85–105. [[CrossRef](#)]
5. Smart, C.C. Artificial tracer techniques for the determination of the structure of conduit aquifers. *Ground Water* **1988**, *26*, 445–453. [[CrossRef](#)]
6. Williams, P.W. The Role of the Subcutaneous Zone in Karst Hydrology. *J. Hydrol.* **1983**, *61*, 45–67. [[CrossRef](#)]
7. Zeng, C.; Liu, Z.H.; Yang, J.W.; Yang, R. A groundwater conceptual model and karst-related carbon sink for a glacierized alpine karst aquifer, Southwestern China. *J. Hydrol.* **2015**, *529*, 120–133. [[CrossRef](#)]
8. Jones, I.C.; Banner, J.L.; Humphrey, J.D. Estimating recharge in a tropical karst aquifer. *Water Resour. Res.* **2000**, *36*, 1289–1299. [[CrossRef](#)]
9. Lee, J.-Y.; Lee, K.-K. Use of hydrologic time series data for identification of recharge mechanism in a fracture bedrock aquifer system. *J. Hydrol.* **2000**, *229*, 190–201. [[CrossRef](#)]
10. Guo, Y.; Qin, D.; Sun, J.; Li, L.; Li, F.; Huang, J. Recharge of River Water to Karst Aquifer Determined by Hydrogeochemistry and Stable Isotopes. *Water* **2019**, *11*, 479. [[CrossRef](#)]
11. Martin, J.B.; Dean, R.W. Exchange of water between conduits and matrix in the Floridan aquifer. *Chem. Geol.* **2001**, *179*, 145–165. [[CrossRef](#)]
12. Massei, N.; Mahler, B.J.; Bakalowicz, M.; Fournier, M.; Dupont, J.P. Quantitative interpretation of specific conductance frequency distributions in karst. *Ground Water* **2007**, *45*, 288–293. [[CrossRef](#)]
13. Aquilina, L.; Ladouche, B.; Doerfliger, N.; Bakalowicz, M. Deep water circulation, residence time, and chemistry in a karst complex. *Ground Water* **2003**, *41*, 790–805. [[CrossRef](#)] [[PubMed](#)]
14. Wong, C.I.; Mahler, B.J.; Musgrove, M.; Banner, J.L. Changes in sources and storage in a karst aquifer during a transition from drought to wet conditions. *J. Hydrol.* **2012**, *468*, 159–172. [[CrossRef](#)]

15. Hanshaw, B.B.; Back, W. Major Geochemical Processes in the Evolution of Carbonate-Aquifer Systems. *J. Hydrol.* **1979**, *43*, 287–312. [[CrossRef](#)]
16. Marfia, A.M.; Krishnamurthy, R.V.; Atekwana, E.A.; Panton, W.F. Isotopic and geochemical evolution of ground and surface waters in a karst dominated geological setting: A case study from Belize, Central America. *Appl. Geochem.* **2004**, *19*, 937–946. [[CrossRef](#)]
17. Ma, R.; Wang, Y.X.; Sun, Z.Y.; Zheng, C.M.; Ma, T.; Prommer, H. Geochemical evolution of groundwater in carbonate aquifers in Taiyuan, northern China. *Appl. Geochem.* **2011**, *26*, 884–897. [[CrossRef](#)]
18. Katz, B.G.; Coplen, T.B.; Bullen, T.D.; Davis, J.H. Use of chemical and isotopic tracers to characterize the interactions between ground water and surface water in mantled karst. *Ground Water* **1997**, *35*, 1014–1028. [[CrossRef](#)]
19. Katz, B.G.; Catches, J.S.; Bullen, T.D.; Michel, R.L. Changes in the isotopic and chemical composition of ground water resulting from a recharge pulse from a sinking stream. *J. Hydrol.* **1998**, *211*, 178–207. [[CrossRef](#)]
20. Wang, Y.; Ma, T.; Luo, Z. Geostatistical and geochemical analysis of surface water leakage into groundwater on a regional scale: A case study in the Liulin karst system, northwestern China. *J. Hydrol.* **2001**, *246*, 223–234. [[CrossRef](#)]
21. Zheng, X.Q.; Zang, H.F.; Zhang, Y.B.; Chen, J.F.; Zhang, F.; Shen, Y. A Study of Hydrogeochemical Processes on Karst Groundwater Using a Mass Balance Model in the Liulin Spring Area, North China. *Water* **2018**, *10*, 903. [[CrossRef](#)]
22. Barbieri, M.; Boschetti, T.; Petitta, M.; Tallini, M. Stable isotope (H-2, O-18 and Sr-87/Sr-86) and hydrochemistry monitoring for groundwater hydrodynamics analysis in a karst aquifer (Gran Sasso, Central Italy). *Appl. Geochem.* **2005**, *20*, 2063–2081. [[CrossRef](#)]
23. Panagopoulos, G.; Lambrakis, N. The contribution of time series analysis to the study of the hydrodynamic characteristics of the karst systems: Application on two typical karst aquifers of Greece (Trifilia, Almyros Crete). *J. Hydrol.* **2006**, *329*, 368–376. [[CrossRef](#)]
24. Qin, D.J.; Zhao, Z.F.; Guo, Y.; Liu, W.C.; Haji, M.; Wang, X.H.; Xin, B.D.; Li, Y.; Yang, Y. Using hydrochemical, stable isotope, and river water recharge data to identify groundwater flow paths in a deeply buried karst system. *Hydrol. Process.* **2017**, *31*, 4297–4314. [[CrossRef](#)]
25. Ma, T.; Wang, Y.; Guo, Q. Response of carbonate aquifer to climate change in northern China: A case study at the Shentou karst springs. *J. Hydrol.* **2004**, *297*, 274–284. [[CrossRef](#)]
26. Zhang, J.; Hao, Y.H.; Hu, B.X.; Huo, X.L.; Hao, P.M.; Liu, Z.F. The effects of monsoons and climate teleconnections on the Niangziguan Karst Spring discharge in North China. *Clim. Dyn.* **2017**, *48*, 53–70. [[CrossRef](#)]
27. Neilson, B.T.; Tennant, H.; Stout, T.L.; Miller, M.P.; Gabor, R.S.; Jameel, Y.; Millington, M.; Gelderloos, A.; Bowen, G.J.; Brooks, P.D. Stream Centric Methods for Determining Groundwater Contributions in Karst Mountain Watersheds. *Water Resour. Res.* **2018**, *54*, 6708–6724. [[CrossRef](#)]
28. Hartmann, A.; Weiler, M.; Wagener, T.; Lange, J.; Kralik, M.; Humer, F.; Mized, N.; Rimmer, A.; Barbera, J.A.; Andreo, B.; et al. Process-based karst modelling to relate hydrodynamic and hydrochemical characteristics to system properties. *Hydrol. Earth Syst. Sci.* **2013**, *17*, 3305–3321. [[CrossRef](#)]
29. Qiao, X.J.; Li, G.M.; Li, Y.P.; Liu, K. Influences of heterogeneity on three-dimensional groundwater flow simulation and wellhead protection area delineation in karst groundwater system, Taiyuan City, Northern China. *Environ. Earth Sci.* **2015**, *73*, 6705–6717. [[CrossRef](#)]
30. De Rooij, R.; Graham, W. Generation of complex karstic conduit networks with a hydrochemical model. *Water Resour. Res.* **2017**, *53*, 6993–7011. [[CrossRef](#)]
31. Scanlon, B.R.; Mace, R.E.; Barrett, M.E.; Smith, B. Can we simulate regional groundwater flow in a karst system using equivalent porous media models? Case study, Barton Springs Edwards aquifer, USA. *J. Hydrol.* **2003**, *276*, 137–158. [[CrossRef](#)]
32. Aquilina, L.; Ladouche, B.; Dorfliger, N. Water storage and transfer in the epikarst of karstic systems during high flow periods. *J. Hydrol.* **2006**, *327*, 472–485. [[CrossRef](#)]
33. Vardanjani, H.K.; Chitsazan, M.; Ford, D.; Karimi, H.; Charchi, A. Initial assessment of recharge areas for large karst springs: A case study from the central Zagros Mountains, Iran. *Hydrogeol. J.* **2018**, *26*, 57–70. [[CrossRef](#)]
34. Moral, F.; Cruz-Sanjulian, J.J.; Olias, M. Geochemical evolution of groundwater in the carbonate aquifers of Sierra de Segura (Betic Cordillera, southern Spain). *J. Hydrol.* **2008**, *360*, 281–296. [[CrossRef](#)]

35. Raeisi, E.; Karami, G. The governing factors of the physicochemical characteristics of Sheshpeer karst springs, Iran. *Carbonate Evaporite* **1996**, *11*, 162–168. [[CrossRef](#)]
36. Aquilina, L.; Ladouche, B.; Dorfliger, N. Recharge processes in karstic systems investigated through the correlation of chemical and isotopic composition of rain and spring-waters. *Appl. Geochem.* **2005**, *20*, 2189–2206. [[CrossRef](#)]
37. Mudarra, M.; Andreo, B.; Baker, A. Characterisation of dissolved organic matter in karst spring waters using intrinsic fluorescence: Relationship with infiltration processes. *Sci. Total Environ.* **2011**, *409*, 3448–3462. [[CrossRef](#)] [[PubMed](#)]
38. Luo, M.M.; Chen, Z.H.; Zhou, H.; Zhang, L.; Han, Z.F. Hydrological response and thermal effect of karst springs linked to aquifer geometry and recharge processes. *Hydrogeol. J.* **2018**, *26*, 629–639. [[CrossRef](#)]
39. Shuster, E.T.; White, W.B. Seasonal fluctuations in the chemistry of limestone springs: A possible means for characterizing carbonate aquifers. *J. Hydrol.* **1971**, *14*, 93–128. [[CrossRef](#)]
40. Kingsbury, J.A. Relation between flow and temporal variations of nitrate and pesticides in two karst springs in northern Alabama. *J. Am. Water Resour. Assoc.* **2008**, *44*, 478–488. [[CrossRef](#)]
41. Atkinson, T.C. Diffuseflow and conduit flow in limestone terrain in the Mendip Hills, Somerset (Great Britain). *J. Hydrol.* **1977**, *35*, 93–110. [[CrossRef](#)]
42. Petelet-Giraud, E.; Luck, J.M.; Ben Othman, D.; Negrel, P. Dynamic scheme of water circulation in karstic aquifers as constrained by Sr and Pb isotopes. Application to the Hérault watershed, Southern France. *Hydrogeol. J.* **2003**, *11*, 560–573. [[CrossRef](#)]
43. Filippini, M.; Squarzone, G.; De Waele, J.; Fiorucci, A.; Vigna, B.; Grillo, B.; Riva, A.; Rossetti, S.; Zini, L.; Casagrande, G.; et al. Differentiated spring behavior under changing hydrological conditions in an alpine karst aquifer. *J. Hydrol.* **2018**, *556*, 572–584. [[CrossRef](#)]
44. Mudarra, M.; Andreo, B. Relative importance of the saturated and the unsaturated zones in the hydrogeological functioning of karst aquifers: The case of Alta Cadena (Southern Spain). *J. Hydrol.* **2011**, *397*, 263–280. [[CrossRef](#)]
45. Bonacci, O. Karst Springs Hydrographs as Indicators of Karst Aquifers. *Hydrol. Sci. J.* **1993**, *38*, 51–62. [[CrossRef](#)]
46. Padilla, A.; Pulidobosch, A.; Mangin, A. Relative Importance of Baseflow and Quickflow from Hydrographs of Karst Spring. *Ground Water* **1994**, *32*, 267–277. [[CrossRef](#)]
47. Dreiss, S.J. Regional Scale Transport in a Karst Aquifer.1. Component Separation of Spring Flow Hydrographs. *Water Resour. Res.* **1989**, *25*, 117–125. [[CrossRef](#)]
48. Dreiss, S.J. Linear Kernels for Karst Aquifers. *Water Resour. Res.* **1982**, *18*, 865–876. [[CrossRef](#)]
49. Scanlon, B.R.; Thrailkill, J. Chemical Similarities among Physically Distinct Spring Types in a Karst Terrain. *J. Hydrol.* **1987**, *89*, 259–279. [[CrossRef](#)]
50. Lakey, B.; Krothe, N.C. Stable isotopic variation of storm discharge from a perennial karst spring, Indiana. *Water Resour. Res.* **1996**, *32*, 721–731. [[CrossRef](#)]
51. Kattan, Z. Environmental isotope study of the major karst springs in Damascus limestone aquifer systems: Case of the Figehe and Barada springs. *J. Hydrol.* **1997**, *193*, 161–182. [[CrossRef](#)]
52. Koeniger, P.; Margane, A.; Abi-Rizk, J.; Himmelsbach, T. Stable isotope-based mean catchment altitudes of springs in the Lebanon Mountains. *Hydrol. Process.* **2017**, *31*, 3708–3718. [[CrossRef](#)]
53. Lamban, L.J.; Jodar, J.; Custodio, E.; Soler, A.; Sapriza, G.; Soto, R. Isotopic and hydrogeochemical characterization of high-altitude karst aquifers in complex geological settings. The Ordesa and Monte Perdido National Park (Northern Spain) case study. *Sci. Total Environ.* **2015**, *506*, 466–479. [[CrossRef](#)]
54. Ryan, M.; Meiman, J. An examination of short-term variations in water quality at a karst spring in Kentucky. *Ground Water* **1996**, *34*, 23–30. [[CrossRef](#)]
55. Nativ, R.; nay, G.G.; Hotzl, H.; Reichert, B.; Solomon, D.K.; Tezcan, L. Separation of groundwater-flow components in a karstified aquifer using environmental tracers. *Appl. Geochem.* **1999**, *14*, 1001–1014. [[CrossRef](#)]
56. Qian, J.Z.; Zhan, H.B.; Wu, Y.F.; Li, F.L.; Wang, J.Q. Fractured-karst spring-flow protections: A case study in Jinan, China. *Hydrogeol. J.* **2006**, *14*, 1192–1205. [[CrossRef](#)]
57. Kang, F.X.; Jin, M.G.; Qin, P.R. Sustainable yield of a karst aquifer system: A case study of Jinan springs in northern China. *Hydrogeol. J.* **2011**, *19*, 851–863. [[CrossRef](#)]
58. Chi, G.; Xing, L.; Zhu, H. The study of quantitative relationship between the spring water and the dynamic change of the atmospheric precipitation in Jinan. *Ground Water* **2017**, *39*, 8–11.

59. Qi, X.F.; Wang, Y.S.; Yang, L.Z.; Liu, Z.Y.; Wang, W.; Li, W.P. Time lag variance of groundwater level response to precipitation of Jinan karst spring watershed in recent 50 years. *Carsol. Sin.* **2016**, *35*, 384–393.
60. Xu, H.Z.; Duan, X.M.; Gao, Z.D.; Wang, Q.B.; Li, W.P.; Yin, X.L. Hydrochemical study of karst groundwater in the Jinan spring catchment. *Hydrogeol. Eng. Geol.* **2007**, *3*, 15–19.
61. Sun, B.; Peng, Y. Boundary condition, water cycle and water environment changes in the Jinan spring region. *Carsol. Sin.* **2014**, *33*, 272–279.
62. Wu, X.; Niu, J.; Niu, J. Experimental research on artificial compensation in Yufu River for groundwater to protect springs. *Water Resour. Power* **2003**, *21*, 53–55.
63. Li, B.; Qin, D.; Guo, Y.; Liu, W.; Haji, M.; Lin, L.; Guan, Q. Effect of Yufu River on chemical processes of karst groundwater in Jinan, Shandong Province. *J. Eng. Geol.* **2017**, *25*, 190–198.
64. Zhou, J. Research on Seepage Field Characteristics of Discharge Area in Jinan Karst Springs. Master's Thesis, University of Jinan, Jinan, China, 2016.
65. Wang, J.L.; Jin, M.G.; Lu, G.P.; Zhang, D.; Kang, F.X.; Jia, B.J. Investigation of discharge-area groundwaters for recharge source characterization on different scales: The case of Jinan in northern China. *Hydrogeol. J.* **2016**, *24*, 1723–1737. [[CrossRef](#)]
66. Partkhurst, D.L.; Appelo, C.A.J. *User's Guide to PHREEQC (Version 2): A Computer Program for Speciation, Batch-Reaction, One-Dimensional Transport and Inverse Geochemical Calculations*; United States Geological Survey: Reston, VA, USA, 1999.
67. Appelo, C.A.J. *Geochemistry, Groundwater and Pollution*; CRC Press: Amsterdam, The Netherlands, 2005.
68. Craig, H. Isotopic Variations in Meteoric Waters. *Science* **1961**, *133*, 1702–1703. [[CrossRef](#)]
69. Grasso, D.A.; Jeannin, P.Y. A global experimental system approach of karst springs' hydrographs and chemographs. *Ground Water* **2002**, *40*, 608–617. [[CrossRef](#)] [[PubMed](#)]
70. Birk, S.; Hergarten, S. Early recession behaviour of spring hydrographs. *J. Hydrol.* **2010**, *387*, 24–32. [[CrossRef](#)]



© 2019 by the authors. Licensee MDPI, Basel, Switzerland. This article is an open access article distributed under the terms and conditions of the Creative Commons Attribution (CC BY) license (<http://creativecommons.org/licenses/by/4.0/>).